LBL-14390

Lawrence Berkeley Laboratory
UNIVERSITY OF CALIFORNIA

Accelerator & Fusion Research Division

Presented at the 1982 Applied Superconductivity Conference, Knoxville, TN, November 28-December 3, 1982; and to be published in the Proceedings

THE SOURCE, ORIGIN AND PROPAGATION OF QUENCHES MEASURED IN SUPERCONDUCTING DIPOLE MAGNETS

S. Caspi and W.V. Hassenzahl

November 1982

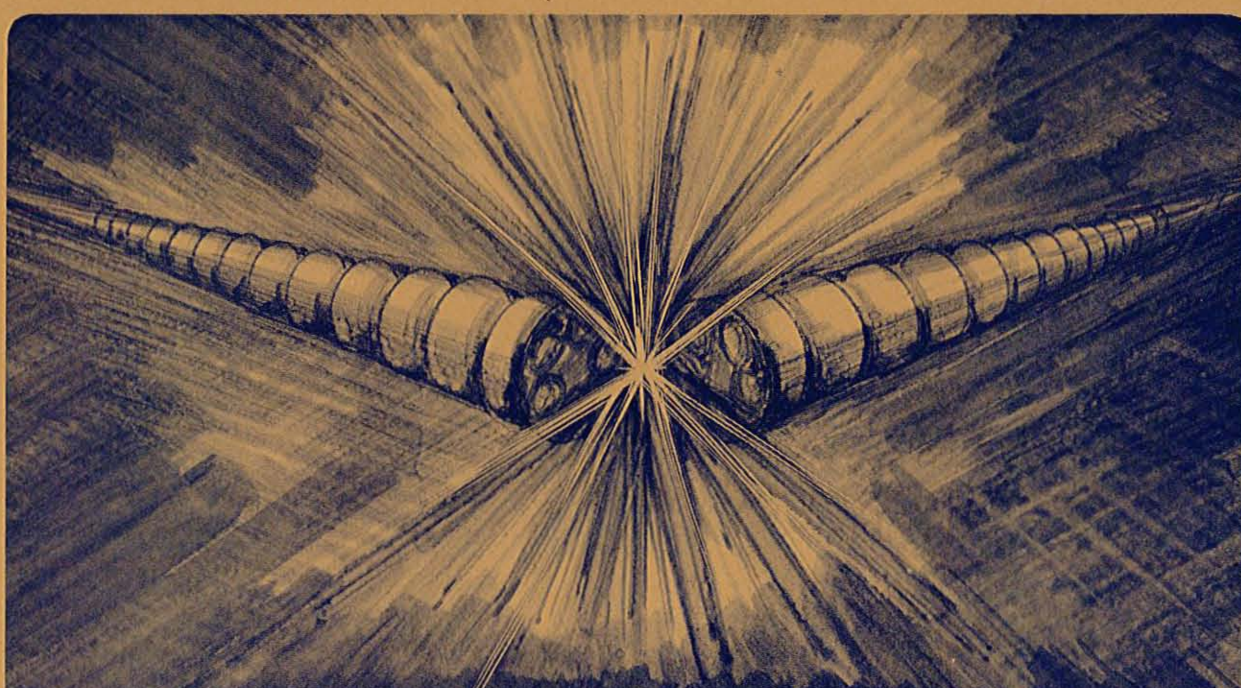

Prepared for the U.S. Department of Energy under Contract DE-AC03-76SF00098

LBL-14390
SUMAG-77

THE SOURCE, ORIGIN AND PROPAGATION OF QUENCHES MEASURED IN SUPERCONDUCTING DIPOLE MAGNETS*

S. Caspi and W. V. Hassenzahl

November 1982

Accelerator and Fusion Research Division
Lawrence Berkeley Laboratory
University of California
Berkeley, California 94720

*This work was supported by the Director, Office of Energy Research, Office of High Energy and Nuclear Physics, High Energy Physics Division, U. S. Dept. of Energy, under Contract No. DE-AC03-76SF00098.

THE SOURCE, ORIGIN AND PROPAGATION OF QUENCHES MEASURED IN SUPERCONDUCTING DIPOLE MAGNETS*

S. Caspi and W. V. Hassenzahl
Lawrence Berkeley Laboratory
University of California
Berkeley, CA 94720

Summary

Transitions from the superconducting to normal state at 4.4 and 1.8 K in several model accelerator dipoles[1,2] were recorded by a fast data acquisition system. The resistive voltage rise in the conductor during the transitions is used to determine accurately the location of the quench source in the magnets and to estimate the axial and turn-to-turn quench velocities. The quench velocity, temperature evolution and energy deposition in the coil were calculated using the program QUENCH,[3] and are in reasonable agreement with the data. In the two dipole magnets studied, the transitions almost always occurred in the regions of highest field. In one coil the high field region is in the straight section because the field in this region is enhanced by iron support rings. In the other magnet the high field region is at the end, in the innermost turn of the first layer. Some quenches were preceded by large voltage spikes that can be ascribed to conductor motion. Other quenches do not appear to be associated with any large energy release. Acoustic emission (AE) was monitored during the tests and AE bursts were observed simultaneous with the initial voltage spike. An increased AE signal continued as the quench progressed.

Introduction

Superconducting dipole magnets in accelerators must operate at high current densities to be economical. Because of the high current density these magnets are not cryostable and most exhibit some training behavior. Very few studies[4] have been made of the quenches in this type of coil as the quench velocities are generally quite high, the point of quench origin is unpredictable, and coil safety usually requires an external protection circuit be engaged as soon as possible after a detectable voltage is observed across the coil. To study transitions in these magnets we acquired a high speed data acquisition system capable of recording up to 16 channels at 10 kHz and used it to monitor coil performance during and preceding quenches. Several channels were used to monitor the voltage across coil sections including fractions of turns in the high field regions, others recorded total coil voltage, and current. All the quenches observed were associated with magnet training and no external disturbances were used to induce quenches.

The inside layer of two model accelerator dipoles were instrumented with voltage taps. The first of these magnets, D-8A, was made of three layers of Mylar- and Kapton-insulated, 23-strand Rutherford cable of the type used for the FNAL doubler. A cross section of one quadrant of the D-8A coil is shown in Fig. 1. The second, D-7H, was a two layer dipole made of the same type of conductor. The inside diameters of the two coils, which have been described elsewhere,[1,2] were 137 mm and 80 mm respectively, corresponding to the sizes of the Brookhaven ISABELLE and the Fermilab doubler/saver coils. The general characteristics of these two coils are presented in Tables I and II and a cross section of the three layer D-8A is shown in Fig. 1.

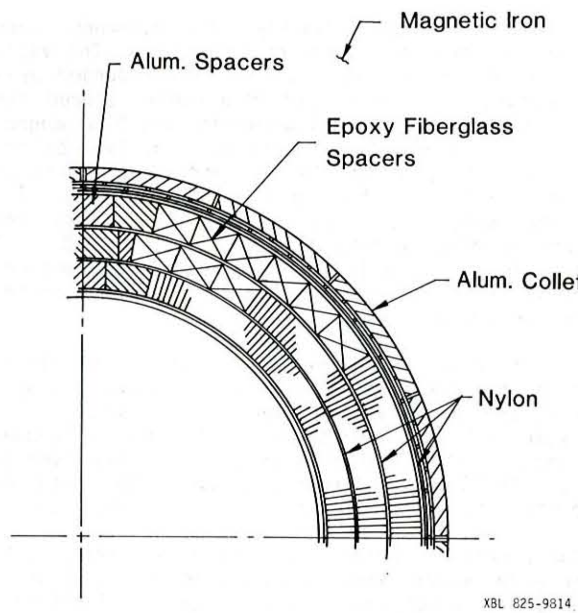

Fig. 1. Cross section of one quadrant of the D-8A coil.

TABLE I: General characteristics of dipole magnet D-8A.

D-8A	Layer 1	Layer 2	Layer 3
Inner radius (mm)	68.7	77.8	87.0
Outer radius (mm)	76.7	85.8	95.0
Turns/quadrant	67	54	35
Angle, top edge of coil (at O.D.)	72.682°	52.179°	30.484°
Angular extent of coil	72.530°	52.043°	30.361°

TABLE II: General characteristics of dipole magnet D-7H

	Layer 1	Layer 2
Inner radius (mm)	40.2	49.0
Outer radius (mm)	50.4	57.0
Turns/quadrant	40	26
Angle, top edge of coil (at O.D.)	69.084°	37.078°
Angular extent of coil	66.366°	36.887°

The larger, D-8A, coil was constrained in the straight sections by iron retaining rings and the D-7H coil had aluminum retaining rings. The iron rings in D-8A give a field enhancement of about 1 T, which caused the high field region to be in the straight section of the coil on the innermost turn

*This work was supported by the Director, Office of Energy Research, Office of High Energy and Nuclear Physics, High Energy Physics Division, U. S. Dept. of Energy, under Contract No. DE-AC03-76SF00098.

Manuscript received November 30, 1982

of the 1st layer. The highest field in the D-7H coil is in the innermost turn of the inner layer at the end of the coil. The retaining rings in both cases are tapered on the inside and slip over collets to provide a circumferential compressive load on the windings. The magnitude of the loads were chosen to ensure compression in the coil at all operating levels. There is some evidence that in D-8A the inner layer was not under compression at the highest operating currents.

Quenches in the Coils

A total of approximately 200 quenches were observed in the dipoles described above. The voltages across various coil sections were recorded by a data acquisition system and permanently stored for later analysis. A typical quench in the D-8A magnet is shown in Figs. 2a, 2b and 2c. In Fig. 2a the measured voltage across the the three inner turns of the north pole is plotted as a function of time. The ordinate, which has units of Ohms, is the measured voltage divided by the quench current, 3100A. A voltage spike, which is ascribed to conductor motion, is followed by a resistive rise as the quench propagates through the coil.

The structure in the resistive rise can be attributed to three effects. The first is axial propagation of the normal region along the conductor in the straight sections. The second is propagation around the ends, and the third is propagation from turn to turn. (No layer to layer propagation was detected prior to enabling the energy extraction circuit.)

The electrical response of the inner turn of the south pole, which remained superconducting, is shown in Fig. 2b. A quiescent period before the initiating voltage spike is followed by a rather noisy period.

Figure 2c shows the raw acoustic emission signal during a quench from a sensor on one of the end rings. The signal is quiescent until the voltage spike of Fig. 2a. At that time a large acoustic burst is observed. This burst is followed by a noisy period that extends beyond the record and probably until well after the current has been reduced to zero by the external protection circuit.

The progression of the quench can be observed in greater detail by looking at short sections of the coil. Figure 3 shows the voltages across sections of the innermost turns of D-7H during a quench. The quench begins in section 6, at one end of the magnet, and progresses towards both straight sections. The slope of the section 6 signal decreases twice (see arrows A an B), as the normal region propagates past a voltage tap. The final slope shows a resistive rise in the section as a result of heating only.

The resistance of the two adjacent sections, 5 and 7, which was initially zero increases as the normal region propagates into them. Note that the initia- tion of the resistive rise in these sections corre- sponds to the inflections in the signal for section 6
(see arrows A and B). Both sections 5 and 7 are observed to be completely normal before the protection circuit is engaged at time = 0, about 38 ms after the quench began.

The locations of most quenches in the two dipoles D-8A and D-7H are shown in Figs. 4a and 4b. Each quench is numbered and enclosed in a box. The quenches in D-8A are almost all in the straight sections, the high field region for this coil. All the

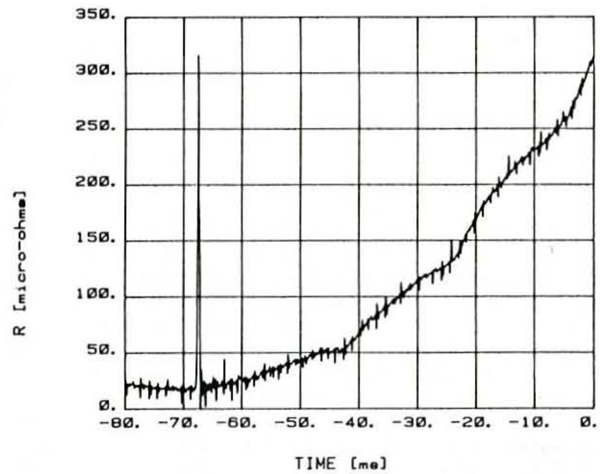

Fig. 2a. Signal observed across a normal going region of the "north pole" of D-8A during a quench.

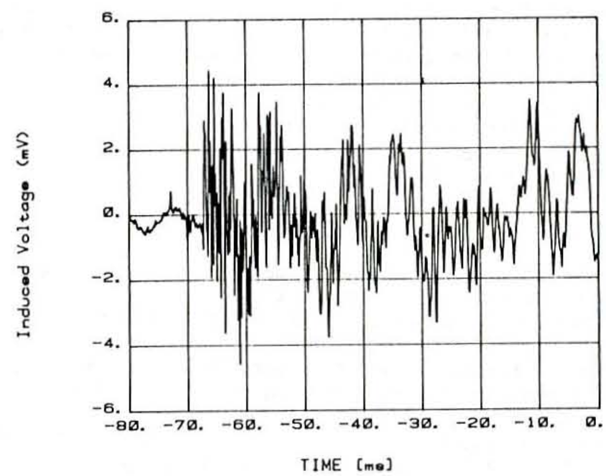

Fig. 2b. Signal observed across the "south" pole of D-8A during the quench shown in Fig. 2a.

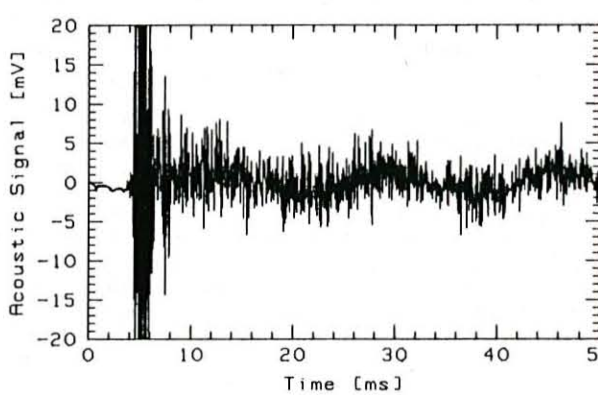

Fig. 2c. Acoustic emission observed during a quench in D-8A.

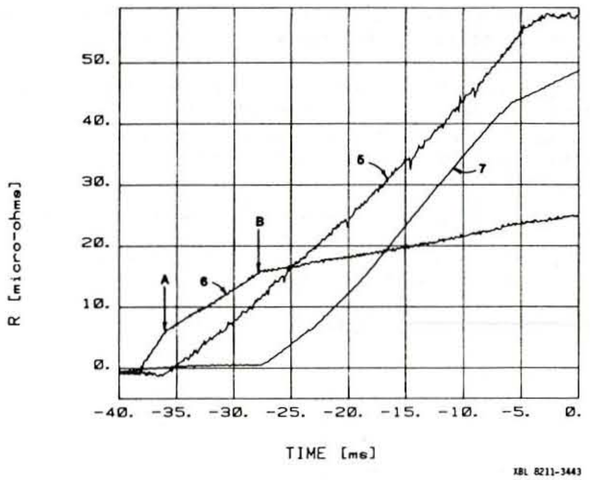

Fig. 3. Normal zone propagation and resistive rise prior to energy extraction. The numbers on the curves correspond to the sections shown in Fig. 4b.

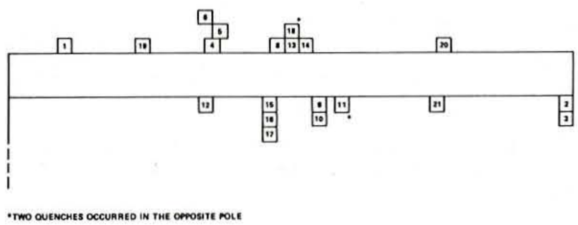

Fig. 4a. Points of quench origin in the innermost turns of the 1st layer of D-8A.

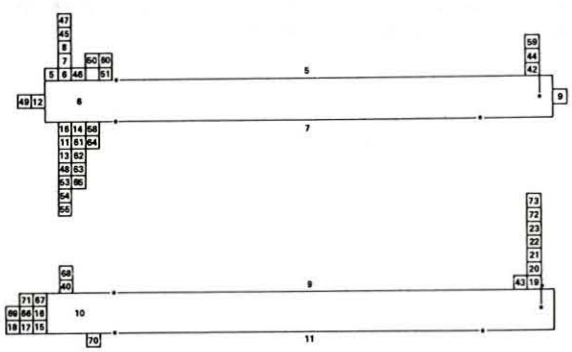

Fig. 4b. Points of quench origin in the inner layer of D-7H. The sequential quench number of these quenches whose origins could be determined precisely are given in the boxes.

quenches in D-7H are at or very near the ends, the high field region.

The voltage response of the coil segments, such as the detailed data of Fig. 3, allows us to calculate the quench propagation velocity. The D-7H magnet was tested in both He I at 4.4 K and He II at 1.8 K and the measured axial quench propagation velocities are shown in Fig. 5a. Velocities between 10 and 70 m/s were observed at both 1.8 and 4.4 K. The limiting value, ~70 m/s, was at a current corresponding almost exactly to the critical current at the bath temperature. Theoretically the velocity should be infinite at the critical current. However, in this coil the fields in the straight sections, where the velocity was measured are about 10% below those at the ends where the quenches start. The measured quench velocities are plotted in Fig. 5b as a function of the ratio of critical current. The velocities in He I and He II nearly overlap when plotted this way.

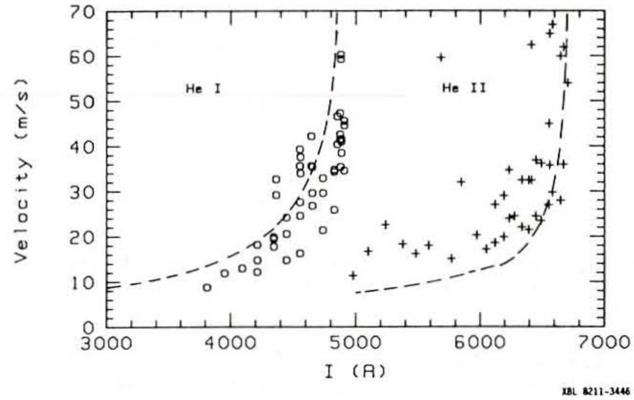

Fig. 5a. Axial quench propagation velocity in D-7H as a function of quench current. The dashed lines are calculated with the program QUENCH.

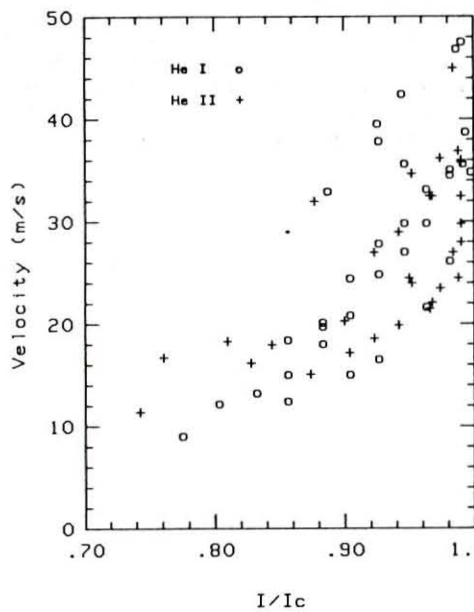

Fig. 5b. Axial quench propagation velocities in D-7H as a function of normalized quench current, quench current divided by short sample current.

The dashed curves of velocities in Fig. 5a were calculated using the program QUENCH with the actual conductor and coil geometry. The calculated velocities depend on the quantity of helium in the conductor cross section. The curves shown in Fig. 5a, which seem to fit the data are based on 3% helium in the conductor cross section, which is within the range of our estimate based on conductor and insulation compaction.

The maximum temperatures in the D-8A coil calculated by the program QUENCH are shown in Fig. 6

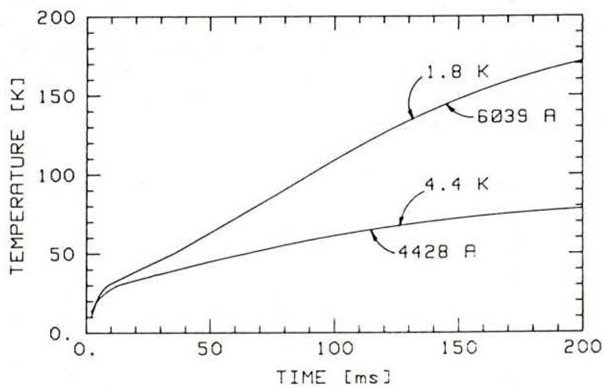

Fig. 6. Temperature response during a quench calculated using the program QUENCH.

for quenches at 90% of critical current. The initial shape of the curve, which appears to have some inflection depends strongly on the helium specific heat, which is assumed to be effectively zero above 20 K. The final temperature, however, is almost independent of the helium contribution.

The turn-to-turn quench propagation is shown in Fig. 7. The time to propagate to the second turn correspond to velocities that are about a factor of 200 less than the axial velocities. Following Wilson[5] this corresponds to the transverse thermal conductivity being about 40,000 times less than the axial thermal conductivity.

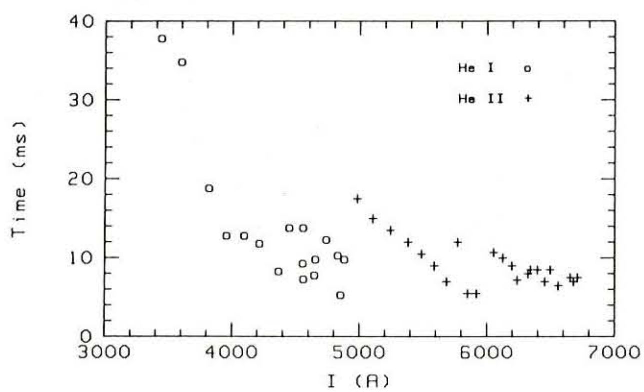

Fig. 7. Transverse quench propagation: transit time from 1st to 2nd turn vs. current.

Quench Initiation

The energy released during the initial voltage spike in some of the quenches in D-8B, a coil that is essentially identical to D-8A except that aluminum rings were used, are presented in Table III. The values of energy indicated are an integral of the product of voltage and current for the duration of the spike and do not reflect any estimate of the distribution of this energy in the coil and the electrical circuit. The quenches in He I were generally triggered by events involving energies about 100 times smaller than those that triggered the quenches in He II. Small disturbances were observed to cause quenches at 4.4 K both before and after the 1.8 K tests. Thus it is evident that the lower energy events must have occurred in He II but they did not cause quenches. The resolution of the detection system before quench #28 was too low to determine the energy released in the precursor. Because the apparatus was only capable of monitoring the coil during a quench, nonquench causing events were not monitored and the maximum safe disturbance cannot be determined.

TABLE III: Energy release in a quench causing event in dipole D-8B.

Quench Number	Current (A)	Temperature (K)	Energy (J)
28	3650	1.75	4.5
31	4075	1.75	6.8
32	4194	1.8	5.1
34	4100	1.8	9.8
43	2910	4.4	0.03
45	2878	4.4	0.11

References

1. S. Caspi, "D-8A-Test Results," LBL Internal Report, SUMAG-58, 1981.

2. S. Caspi, "D-7H-Test Results," LBL Report 14796, 1982.

3. W. Hassenzahl, "Quench - Modifications and Documentation," CEN SACLAY Report SUPRA/78-61 CEN, 1978.

4. M. Garber and W. B. Sampson, "Quench Properties of High Current Superconductors," IEEE Trans. Magn. MAG-15, 77, 1981.

5. M. N. Wilson, "Computer Simulation of the Quenching of a Superconducting Magnet," Rutherford High Energy Lab., Report RHEL/M 151.